



Instituto Nacional de Saúde
Doutor Ricardo Jorge



Fundação
para a Ciência
e a Tecnologia

Modelling Mobility Data during COVID-19 in Portugal with R-INLA

XXVII Congresso SPE 25, October 25

André Brito^{1,2,3}, Ausenda Machado^{3,4}, Ana Paula Rodrigues³, Paula Patrício^{1,2}, Regina Bispo^{2,5}

¹Department of Mathematics, NOVA School of Science and Technology (NOVA FCT), Lisbon, Portugal

²Center for Mathematics and Applications (NOVA Math), Lisbon, Portugal

³Department of Epidemiology, National Institute of Health Dr. Ricardo Jorge, Lisbon, Portugal

⁴Comprehensive Health Research Center (CHRC), NOVA University Lisbon, Portugal

⁵School of Mathematics and Statistics and Centre for Research into Ecological and Environmental Modelling University of St Andrews, St. Andrews, UK

Introduction

- Human mobility was severely disrupted during the COVID-19 pandemic, as restrictions and behavioural shifts led to **unprecedented movement patterns** [1].
- Mobility data can act as a proxy for interpersonal contact and transmission risk, supporting the design of **adaptive mitigation measures**. Yet, behavioural adaptations may **weaken this proxy relationship** [2].
- Regression analyses indicate that mobility effectively predicted weekly COVID-19 infection rates during the first wave [3], and that **reduced mobility during the Omicron surge lowered peak incidence** [4].
- Integrating mobility data into epidemic models—particularly in early pandemic stages—**improved predictive accuracy** and **enhanced variant tracking**, outperforming models that ignored travel or used lagged indicators [5].

Objectives

Aim: To model district-level mobility data from the **COVID-19 Google Community Mobility Reports** for Portugal [6].

Specific objectives:

1. **Describe** mobility patterns and the **movement stringency** dynamics during the COVID-19 pandemic in Portugal.
2. **Build** a comprehensive dataset with **key predictors** explaining mobility variability.
3. **Develop and evaluate** time series models to accurately capture mobility trends.
4. **Identify** significant predictors and **characterize their effects** across mobility categories and districts.
5. **Assess** the impact of **stringency measures** on observed mobility.

Data

Google's COVID-19 Community Mobility Reports (CMR) [6]

Derived from Google Location Services (e.g., Google Maps), covering multiple countries — including Portugal — and span from **February 15, 2020 to October 15, 2022**, across different spatial levels of detail.

- Data represent the **percentage change in mobility** relative to a pre-pandemic **baseline**, across six location categories:
 - Retail and Recreation
 - Grocery and Pharmacy
 - Parks
 - Transit Stations
 - Workplaces
 - Residential
- The **baseline** is defined as the **median mobility value for each weekday** during the period **January 3–February 6, 2020**, when mobility restrictions were not yet in place.

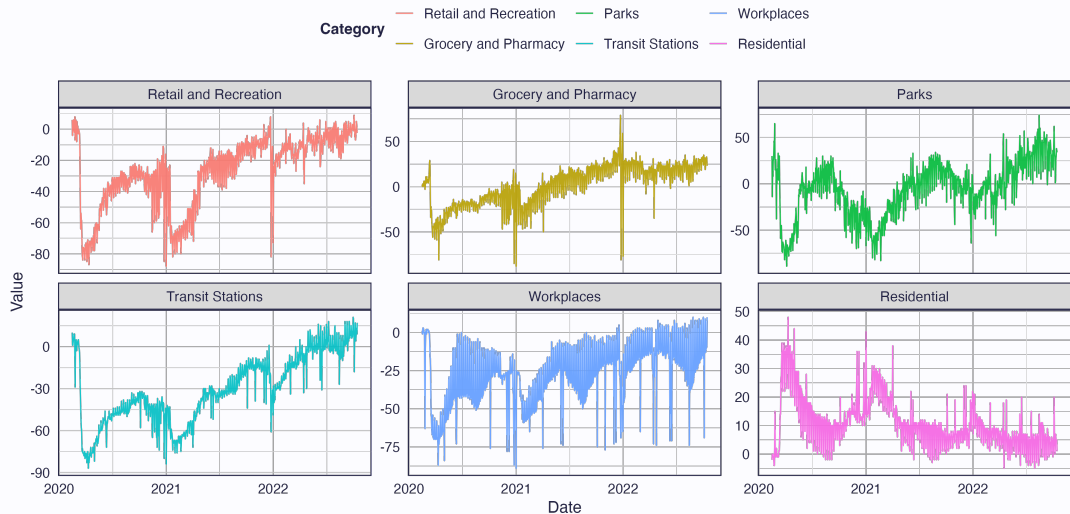


Figure 1: Overall mobility for mainland Portugal for all six categories.

During the COVID-19 pandemic, **Portugal and other countries** imposed movement restrictions, which were adjusted based on the **evolving situation**.

Movement Stringency Index [7]

Numerical score quantifying the effect of public health measures on movement restriction.

Based on nine metrics: **school, workplace, and transport closures, public event cancellations, gathering restrictions**, stay-at-home orders, public information campaigns, internal movement restrictions, and international travel controls.

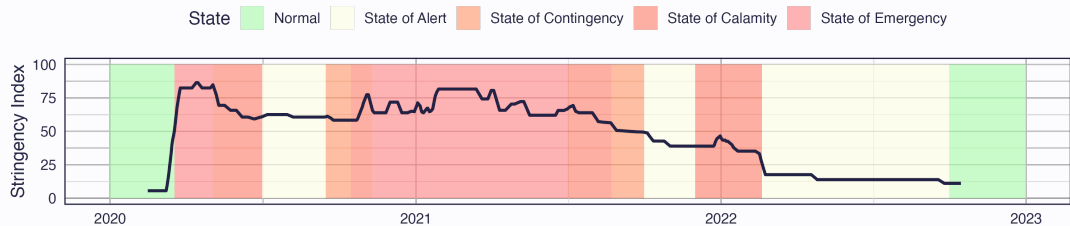


Figure 2: Movement stringency index overlaid on the Exceptional Legal Regime in force coded by colour.

Climate Data Store (CDS) [8]

Operated by the **Copernicus Climate Change Service (C3S)**, provides free and open access to high-quality climate datasets – including **daily gridded temperature observations** across Europe.

- Higher temperatures have been associated with a **lower incidence of COVID-19** [9].
- Temperature variations may also **influence mobility patterns** over time, serving as an important explanatory variable.

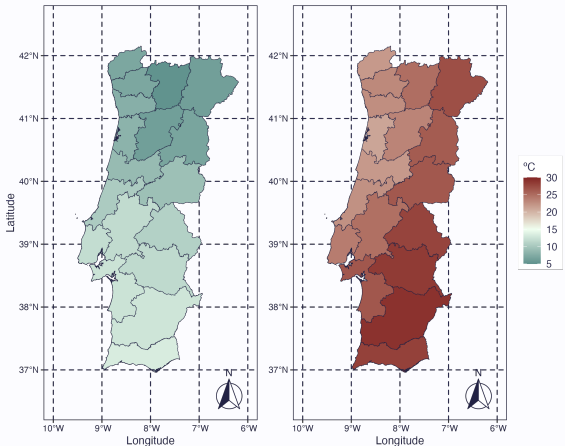


Figure 3: Mean temperature values on February 18th 2020 and August 15th 2021 per District.

- Clear weekly patterns emerge, particularly in:
 - Workplaces
 - Transit Stations
 - Retail & Recreation
- National holidays cause notable deviations in mobility, especially during weekdays.

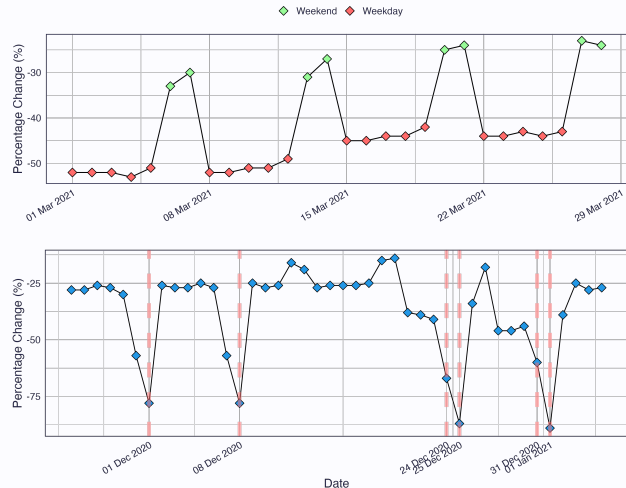


Figure 4: Percentage change in the Workplaces mobility category over time.

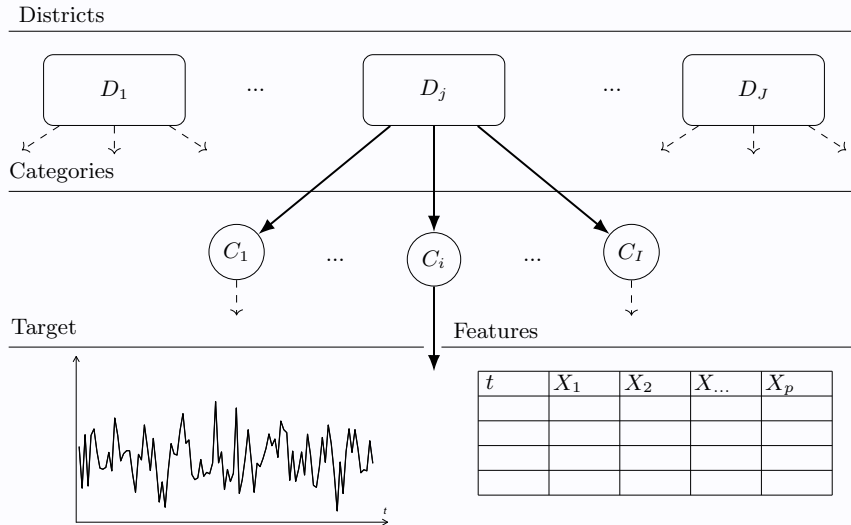


Figure 5: Schematic representation of the hierarchical dataset structure. For each District–Category pair (D_j, C_i) , where $j = 1, \dots, J$ and $i = 1, \dots, I$, there is an associated distinct target time series and a set of features X_1, \dots, X_p , which may vary across time, space, or both. The representation is the same for each District-Category represented by the dashed lines.

Model

Hierarchical models break the modelling process into stages (1) *Observations*; (2) *Process*, and (3) *Parameters* [10].

Latent Gaussian Models (LGM) are Bayesian hierarchical models with a Gaussian assumption on the latent parameters. These include a wide and flexible class of models, namely, spatial and spatio-temporal models.

INLA (Integrated Nested Laplace Approximation) is a fast alternative for LGM.

Hierarchical Model Structure [11]:

$$(1) \mathbf{y} | \mathbf{x}, \boldsymbol{\theta} \sim \pi(y_i | x_i, \boldsymbol{\theta}) \quad (i = 1, \dots, n), \quad (2) \mathbf{x} | \boldsymbol{\theta} \sim \mathcal{N}(\mathbf{0}, \mathbf{Q}^{-1}(\boldsymbol{\theta})), \quad (3) \boldsymbol{\theta} \sim \pi(\boldsymbol{\theta})$$

- \mathbf{y} is the vector containing the observations (response),
- \mathbf{x} is the vector containing the latent parameters, i.e., represents the latent Gaussian field,
- $\boldsymbol{\theta}$ is a vector of hyperparameters,
- $\mathbf{Q}(\boldsymbol{\theta})$ is the precision matrix (i.e., the inverse of the covariance matrix).

The aim is to model mobility over three categories - Workplaces (C_1), Retail and Recreation (C_2), and Transit Stations (C_3) - across mainland Portugal using daily time data grouped per district.

$$Y_{jtc} = \beta_c + \text{temporal}_{jtc} + \text{lockdown}_{tc} + \text{stringency}_t + \text{temperature}_{jt} + u_j + v_j + \gamma_{t|c} + \phi_{t|c} + \delta_{jt|c}$$

where,

- Y_{jtc} is the percentage change in mobility for district j ($j = 1, \dots, 18$) on day t for category c ($c = C_1, C_2, C_3$) and β_c represents a fixed effect per category.
- Random effects c ,

$$\underbrace{u_j + v_j}_{\text{spatial effects}} + \underbrace{\gamma_{t|c} + \phi_{t|c}}_{\text{temporal effects}} + \underbrace{\delta_{jt|c}}_{\text{space-time interaction}} \quad [10]$$

$$Y_{jtc} = \beta_c + \text{temporal}_{jtc} + \text{lockdown}_{tc} + \text{stringency}_t + \text{temperature}_{jt} + u_j + v_j + \gamma_{t|c} + \phi_{t|c} + \delta_{j|t|c}$$

- β_c – category-specific fixed effects $\beta_c = \sum_{i=1}^3 \beta_{C_i} \mathbb{I}(c = C_i)$.
- $\text{temporal}_{j,t,c}$ – category-specific linear trends, Fourier terms, day of the week and district holiday indicators.
- $\text{lockdown}_{t,c}$ – full lockdown indicator with category-specific random effects.
- stringency_t – national movement stringency index [7]).
- temperature_{jt} – daily mean temperature for district j on day t , with fixed and district-specific random effects.
- $u_j + v_j$ – spatial effects modeled using the Besag–York–Molli   (BYM) model [12, 11].
- $\gamma_{t|c}$ – correlated random temporal effect by mobility category c .
- $\phi_{t|c}$ – uncorrelated temporal effect by category c .
- $\delta_{j|t|c}$ – Type I space–time interaction, combining unstructured spatial and temporal effects.

- Training set: **Feb 20, 2020 – Feb 20, 2022**; Testing set: **Feb 21, 2022 – Oct 15, 2022** (\approx 75–25% train-test split).
- Models were estimated using the **R-INLA** package [13].
- Model fit was evaluated with **DIC** and **WAIC**, while predictive performance was assessed using **MAE** and **RMSE** on both training and test sets [10, 14].

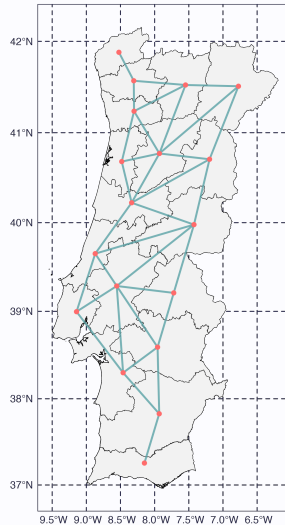


Figure 6: Geographical representation of mainland Portugal's districts with overimposed adjacency graph.

Results

Results

Table 1: Model specification and fit statistics

Model	DIC	WAIC	MSE (Train)	RMSE (Train)	MSE (Test)	RMSE (Test)
model	260647.71	278280.91	5.89	9.21	19.98	27.35

Table 2: Posterior estimates for the model, mean, standard deviation (SD), quantiles at 2.5%, 50% and 97.5%, and mode.

Covariate	Coefficient	Mean	SD	Q 2.5%	Q 50%	Q 97.5%	Mode
category	β_{c_1}	-15.76	5.46	-26.56	-15.73	-5.14	-15.73
category	β_{c_2}	22.38	5.39	11.84	22.36	33.03	22.36
category	β_{c_3}	15.52	5.28	5.26	15.49	25.97	15.49
temporal features	α
dow [Saturday]	η_{d_2}	-0.30	1.19	-2.64	-0.30	2.05	-0.30
dow [Sunday]	η_{d_3}	-0.34	2.22	-4.71	-0.34	4.02	-0.34
national holiday	θ_1	-29.47	1.25	-31.92	-29.47	-27.01	-29.47
regional holiday	θ_2	-6.78	1.35	-9.44	-6.78	-4.13	-6.78
commemorative holiday	θ_3	-12.99	2.01	-16.94	-12.99	-9.05	-12.99
lockdown	ψ	-12.02	2.77	-17.49	-12.02	-6.56	-12.02
stringency	ζ	-0.77	0.03	-0.83	-0.77	-0.72	-0.77
temperature	ω	0.68	0.17	0.35	0.68	1.02	0.68

Results

Table 3: Posterior estimates for the model hyperparameters, posterior mean, posterior standard deviation (SD), quantiles at 2.5%, 50% and 97.5%, and Mode.

Covariate	Parameter	Mean	SD	Q 2.5%	Q 50%	Q 97.5%	Mode
fixed effects	τ	0.01	0.00	0.01	0.01	0.01	0.01
dow	τ_η	0.02	0.00	0.01	0.02	0.02	0.02
lockdown	τ_ψ	0.06	0.02	0.02	0.06	0.12	0.06
temperature	τ_ω	2.33	0.52	1.48	2.27	3.53	2.16
spatial comp.	τ_u	283.67	139.87	69.91	261.17	596.34	200.66
unstructured comp.	τ_v	0.01	0.00	0.01	0.01	0.02	0.01
AR time effect (AR1)	τ_γ	0.01	0.00	0.01	0.01	0.01	0.01
correlation term (AR1)	ρ	0.98	0.00	0.98	0.99	0.99	0.99
time effect	τ_ϕ	0.02	0.00	0.02	0.02	0.02	0.02
space-time interaction	τ_δ	2.06	3.13	0.38	1.16	9.61	0.54

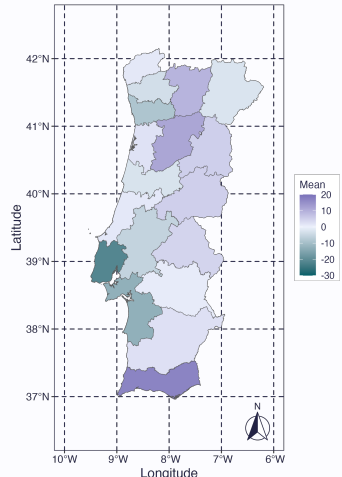


Figure 7: Posterior mean of the structured spatial main effect $u_j + v_j$.

Results

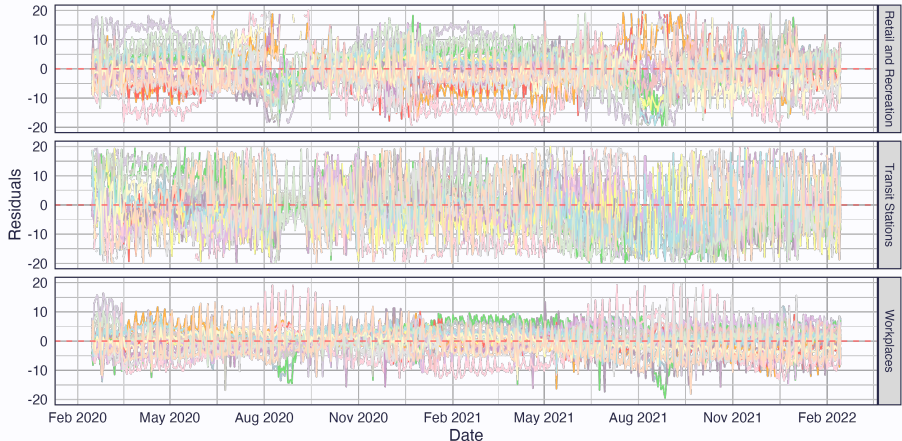


Figure 8: Time series of the residuals per category of mobility for training data coloured by district (each line).

Results

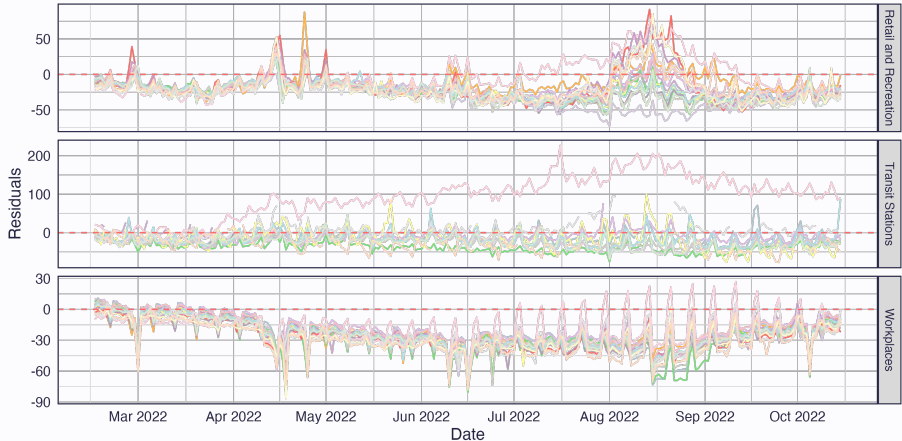


Figure 9: text

Results

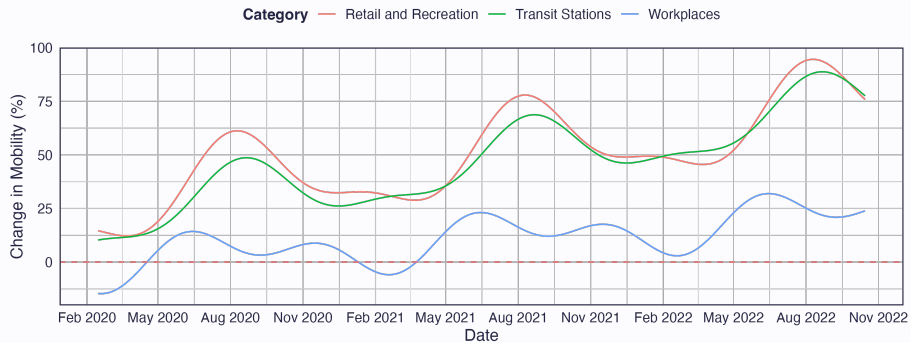


Figure 10: Time series of the underlying mobility seasonal patterns, baseline B_{C_f} , linear and Fourier terms, per category.

Discussion

Discussion

- Fourier terms and **linear trends** significantly capture the **seasonal patterns** of each mobility category.
- **Holiday indicators** are highly significant, especially in the **Workplace category**, for capturing mobility disruptions.
- **Stringency** and **lockdown measures** jointly **reduce mobility**, with lockdowns amplifying the effects of stricter restrictions; however, the **stringency index alone is insufficient to capture abrupt changes**.
- Entering a **full lockdown** leads to an average **12% reduction** in mobility across all categories.
- Temperature has a **small but significant positive effect**, increasing mobility by approximately **0.68% per degree rise**.

References

References i

- [1] Riccardo Gallotti, Filippo Valle, Nicola Castaldo, Pierluigi Sacco, and Manlio De Domenico.
Unprecedented disruption of human mobility and daily activities during the covid-19 pandemic.
Scientific Reports, 11(1):1-12, 2021.
- [2] Pierre Nouvellet, Sangeeta Bhatia, Anne Cori, Kylie E.C. Ainslie, Marc Baguelin, Samir Bhatt, Adhiratha Boonyasiri, Nicholas F. Brazeau, Lorenzo Cattarino, Laura V. Cooper, Helen Coupland, Zulma M. Cucunuba, Gina Cuomo-Dannenburg, Amy Dighe, Bimandra A. Djafara, Ilaria Dorigatti, Oliver D. Eales, Sabine L. van Elsland, Fabricia F. Nascimento, Richard G. FitzJohn, Katy A.M. Gaythorpe, Lily Geidelberg, William D. Green, Arran Hamlet, Katharina Hauck, Wes Hinsley, Natsuko Imai, Benjamin Jeffrey, Edward Knock, Daniel J. Laydon, John A. Lees, Tara Mangal, Thomas A. Mellan, Gemma Nedjati-Gilani, Kris V. Parag, Margarita Pons-Salort, Manon Ragonnet-Cronin, Steven Riley, H. Juliette T. Unwin, Robert Verity, Michaela A.C. Vollmer, Erik Volz, Patrick G.T. Walker, Caroline E. Walters, Haowei Wang, Oliver J. Watson, Charles Whittaker, Lilith K. Whittles, Xiaoyue Xi, Neil M. Ferguson, and Christl A. Donnelly.
Reduction in mobility and covid-19 transmission.
Nature Communications, 12, 12 2021.
- [3] Josiah L. Kephart, Xavier Delclòs-Aliò, Daniel A. Rodríguez, Olga L. Sarmiento, Tonatiuh Barrientos-Gutiérrez, Manuel Ramírez-Zea, D. Alex Quistberg, Usama Bilal, and Ana V. Diez Roux.
The effect of population mobility on covid-19 incidence in 314 latin american cities: a longitudinal ecological study with mobile phone location data.
The Lancet Digital Health, 3:e716–e722, 11 2021.
- [4] Justin Elarde, Joon Seok Kim, Hamdi Kavak, Andreas Züfle, and Taylor Anderson.
Change of human mobility during covid-19: A united states case study.
PLoS ONE, 16, 11 2021.
- [5] M. Sulyok and M. Walker.
Community movement and covid-19: A global study using google's community mobility reports.
Epidemiology and Infection, 2020.
- [6] Google LLC.
Covid-19 community mobility reports.
<https://www.google.com/covid19/mobility/>, 2020.
Accessed: 2024-09-02.
- [7] University of Oxford – with minor processing by Our World in Data Blavatnik School of Government.
Covid-19 containment and health index [dataset].
<https://ourworldindata.org/grapher/covid-containment-and-health-index>, 2023.
Government Response Tracker (OxCGR) [original data].

References ii

- [8] Copernicus Climate Change Service (C3S).
In-situ gridded observations for europe, 2025.
Accessed: 2025-02-19.
- [9] Luise Nottmeyer, Ben Armstrong, Rachel Lowe, Sam Abbott, Sophie Meakin, Kathleen M. O'Reilly, Rosa von Borries, Rochelle Schneider, Dominic Royé, Masahiro Hashizume, Mathilde Pascal, Aurelio Tobias, Ana Maria Vicedo-Cabrera, Eric Lavigne, Patricia Matus Correa, Nicolás Valdés Ortega, Jan Kynčl, Aleš Urban, Hans Orru, Niilo Rytí, Jouni Jaakkola, Marco Dallavalle, Alexandra Schneider, Yasushi Honda, Chris Fook Sheng Ng, Barrak Alahmad, Gabriel Carrasco-Escobar, Julian Horia Holobâc, Ho Kim, Whanhee Lee, Carmen Iñiguez, Michelle L. Bell, Antonella Zanobetti, Joel Schwartz, Noah Scovronick, Micheline de Sousa Zanotti Staglorio Coêlho, Paulo Hilario Nascimento Saldiva, Magali Hurtado Diaz, Antonio Gasparrini, and Francesco Sera.
The association of covid-19 incidence with temperature, humidity, and uv radiation – a global multi-city analysis.
Science of the Total Environment, 854, 1 2023.
- [10] Marta Blangiardo and Michela Cameletti.
Spatial and Spatio-temporal Bayesian Models with R-INLA.
John Wiley & Sons, Chichester, West Sussex, 2015.
- [11] Paula Moraga.
Spatial Statistics for Data Science: Theory and Practice with R.
Chapman & Hall/CRC, 2023.
- [12] Julian Besag, Jeremy York, and Annie Mollii.
*Bayesian image restoration, with two applications in spatial statistics** **.
Technical report, 1991.
- [13] Finn Lindgren and Håvard Rue.
Bayesian spatial modelling with r-inla.
Journal of Statistical Software, 63(19):1–25, 2015.
- [14] Sumio Watanabe SWATANAB.
Asymptotic equivalence of bayes cross validation and widely applicable information criterion in singular learning theory.
Technical report, 2010.

Thank you for your attention

Any questions?

This work is funded by national funds through the FCT – Fundação para a Ciência e a Tecnologia, I.P., under the scope of the projects UIDB/00297/2020 (<https://doi.org/10.54499/UIDB/00297/2020>), UIDP/00297/2020 (<https://doi.org/10.54499/UIDP/00297/2020>) (Center for Mathematics and Applications) and 2024.00664.BDANA



$$\gamma_{jtc} = \beta_c + \text{temporal}_{jtc} + \text{lockdown}_{tc} + \text{stringency}_t + \text{temperature}_{jt} + u_j + v_t + \gamma_{t|c} + \phi_{t|c} + \delta_{jt|c}$$

Exploring each term in detail:

- β_c includes category fixed effect terms,

$$\beta_c = \sum_{i=1}^3 \beta_{C_i} \mathbb{I}(c = C_i) \quad (1)$$

where $\mathbb{I}(c = C_i)$ is the indicator function that takes the value 1 if c is the category C_i , and 0 otherwise.

$$\gamma_{jtc} = \beta_c + \text{temporal}_{jtc} + \text{lockdown}_{tc} + \text{stringency}_t + \text{temperature}_{jt} + u_j + v_j + \gamma_{t|c} + \phi_{t|c} + \delta_{jt|c}$$

- The temporal_{jtc} covariates include

$$\begin{aligned}\text{temporal}_{jtc} = & \sum_{i=1}^3 \left[\mathbb{I}(c = C_i) \left(\alpha_{C_i 0} t + \alpha_{C_i 1} \cos\left(\frac{2\pi}{365.25} t\right) + \right. \right. \\ & \left. \left. \alpha_{C_i 2} \sin\left(\frac{2\pi}{365.25} t\right) + \alpha_{C_i 3} \sin\left(\frac{4\pi}{365.25} t\right) + \alpha_{C_i 4} \sin\left(\frac{4\pi}{365.25} t\right) \right) \right] + \\ & \sum_{k=1}^3 (\eta_{d_k} + \tilde{\eta}_{d_k j c}) \mathbb{I}(\text{dow}_t = d_k) + \\ & \theta_1 \text{national holiday}_t + \theta_2 \text{regional holiday}_{tj} + \theta_3 \text{commemorative holiday}_t\end{aligned}$$

$$\gamma_{jtc} = \beta_c + \text{temporal}_{jtc} + \text{lockdown}_{tc} + \text{stringency}_t + \text{temperature}_{jt} + u_j + v_j + \gamma_{t|c} + \phi_{t|c} + \delta_{jt|c}$$

- the lockdown_{tc} term is an indicator variable to identify the periods under full lockdown. The term also includes category-specific random effects,

$$\text{lockdown}_{tc} = (\psi + \tilde{\psi}_c) \mathbb{I}(t \in L)$$

with L being the time intervals from March 18th to May 2nd 2020 and from January 14th to March 14th 2021.

$$Y_{jtc} = \beta_c + \text{temporal}_{jtc} + \text{lockdown}_{tc} + \text{stringency}_t + \text{temperature}_{jt} + u_j + v_j + \gamma_{t|c} + \phi_{t|c} + \delta_{jt|c}$$

- the **stringency_t** term is the national movement stringency index developed by Hale *et al.* [7] across all categories and districts,

$$\text{stringency}_t = \zeta \text{stringency}_t$$

$$Y_{jtc} = \beta_c + \text{temporal}_{jtc} + \text{lockdown}_{tc} + \text{stringency}_t + \text{temperature}_{jt} + u_j + v_j + \gamma_{t|c} + \phi_{t|c} + \delta_{jt|c}$$

- the temperature_{jt} term includes the daily mean temperature computed for the district j at day t . The mean temperature is used as it comprises the 24 hour exposure of the individuals. It includes a fixed effect combined with a district-specific random effects,

$$\text{temperature}_{jt} = (\omega + \tilde{\omega}_j) \text{ temperature}_{jt} \quad (2)$$

$$Y_{jtc} = \beta_c + \text{temporal}_{jtc} + \text{lockdown}_{tc} + \text{stringency}_t + \text{temperature}_{jt} + u_j + v_j + \gamma_{t|c} + \phi_{t|c} + \delta_{jt|c}$$

u_j represents the structured district-specific spatial effect, it is an intrinsic conditional autoregressive (iCAR) structure, which captures spatial dependences using the neighbourhood structure of the spatial units [10]. Assuming n areas, each having its own set of neighbours $\mathcal{N}(j)$, u_j is defined as,

$$u_j | \mathbf{u}_{-j} \sim N \left(\mu_j + \frac{1}{\mathcal{N}_j} \sum_{m=1}^n a_{mj} (u_m - \mu_m), s_j^2 \right) \quad (j = 1, \dots, 18)$$

where μ_j and $s_j^2 = \sigma_u^2 / \mathcal{N}_j$ are the mean and variance for area j , respectively, and $\mathbf{u}_{-j} = \{u_1, \dots, u_{j-1}\}$. The variance depends on the number neighbours for area j - the higher the number of neighbours the smaller the variance. The quantity a_{ij} takes value 1 if areas i and j are neighbours.

$$Y_{jtc} = \beta_c + \text{temporal}_{jtc} + \text{lockdown}_{tc} + \text{stringency}_t + \text{temperature}_{jt} + u_j + v_j + \gamma_{t|c} + \phi_{t|c} + \delta_{jt|c}$$

- v_j represents an unstructured component that accounts for the residual spatial variation modelled by an a prior Normal distribution $v_j \sim N(0, 1/\tau_v)$ with precision $\tau_v \sim \text{Gamma}(1, 0.001)$. The $u_j + v_j$ specification constitutes the Besag–York–Molliè (BYM) model [12, 11].

$$Y_{jtc} = \beta_c + \text{temporal}_{jtc} + \text{lockdown}_{tc} + \text{stringency}_t + \text{temperature}_{jt} + u_j + v_j + \gamma_{t|c} + \phi_{t|c} + \delta_{jt|c}$$

- $\gamma_{t|c}$ represents a correlated random time effect given a category of mobility c , it accounts for time dependencies conditional on the category. This component assumes that the mobility for a given district in a given day depends on the mobility on the previous day. This is modelled as an autoregressive process such that

$$\gamma_{1|c} \sim N\left(0, (\tau_\gamma(1 - \rho^2))^{-1}\right)$$

$$\gamma_{t|c} = \rho \gamma_{t-1|c} + \epsilon_{t|c}$$

$$\epsilon_{t|c} \sim N\left(0, \frac{1}{\tau_\gamma}\right)$$

where the precision term $\tau_\gamma \sim \text{Gamma}(1, 0.001)$ and ρ represents a temporal correlation term.

$$Y_{jtc} = \beta_c + \text{temporal}_{jtc} + \text{lockdown}_{tc} + \text{stringency}_t + \text{temperature}_{jt} + u_j + v_j + \gamma_{t|c} + \phi_{t|c} + \delta_{jt|c}$$

- $\phi_{t|c}$ represents an uncorrelated time dependence given a category c that accounts for independent time effects. This uncorrelated time effect is modelled by a normal distribution with zero mean value and precision τ_ϕ ,

$$\phi_{t|c} \sim N\left(0, \frac{1}{\tau_\phi}\right)$$

where $\tau_\phi \sim \text{Gamma}(1, 0.001)$.

- $\delta_{jt|c}$ represents the space time interaction term, conditional to a category c . In this work, it is defined as a Type I space-time interaction - Type I assumes the two unstructured spatial and temporal effects interact.